Phonon properties of the spinel oxide $MgTi_2O_4$ with the $S=1/2$ pyrochlore lattice

Z. V. Popović,[1,2] G. De Marzi,[1] M. J. Konstantinović,[3] A. Cantarero,[1] Z. Dohčević-Mitrović,[2] M. Isobe,[4] and Y. Ueda[4]
[1]*Materials Science Institute, University of Valencia, P.O. Box 22085, 46071 Valencia, Spain*
[2]*Institute of Physics, P.O. Box 68, 11080 Belgrade, Serbia*
[3]*Laboratorium voor Vaste-Stoffysica en Magnetisme, Katholieke Universiteit Leuven, Celestijnenlaan 200D, B-3001 Leuven, Belgium*
[4]*Materials Design and Characterization Laboratory, Institute for Solid State Physics, The University of Tokyo, 5-1-5 Kashiwanoha, Kashiwa, Chiba 277-8581, Japan*

(Received 24 February 2003; revised manuscript received 18 June 2003; published 10 December 2003)

We study the phonon dynamics of $MgTi_2O_4$ spinel by measuring the Raman and infrared reflectivity spectra in a wide frequency (100–3000 cm^{-1}) and temperature (10 K–300 K) range. The reflectivity spectra are analyzed by a fitting procedure based on a model which includes both Drude and phonon oscillator contributions to the dielectric constant. The phonon assignment is done from comparison between experimental data and shell model lattice dynamical calculations. We find two infrared-active F_{1u} symmetry modes superimposed on the free carrier continuum, and four Raman-active modes of $1A_{1g}$, $1E_g$, and $2F_{2g}$ symmetry. At the phase transition temperature of about 250 K we observe an abrupt change of optical parameters, accompanied with the appearance of new phonon modes.

DOI: 10.1103/PhysRevB.68.224302 PACS number(s): 78.30.Hv, 64.70.Kb, 63.20.Dj, 78.20.Ci

I. INTRODUCTION

The spinel oxides AB_2O_4 are one of the richest family referring to the number of compounds and variety of observed physical properties, such as superconductivity,[1] heavy fermion behavior,[2] charge ordering,[3] and unusual magnetic properties.[4,5] The unique structural character of the cubic spinel structure is a three-dimensional (3D) network of corner-sharing tetrahedra formed by B cations (pyrochlore lattice), Fig. 1. Such geometry of the crystal lattice produces a strong frustration in the electron interactions, which is usually released at low temperatures through a structural phase transition. Simultaneously, the long-range antiferromagnetic (AF) ordering takes place.[4,5] Interestingly, in the extreme quantum case, the ground state of the $S=1/2$ Heisenberg AF on a pyrochlore lattice is predicted to be a quantum spin liquid[6] instead. However, this picture can be drastically altered by allowing the coupling between spins and phonons,[7,8] so that the system may relax either into quasi-long-range bond-ordered phase or to standard Néel phase.

One of the compounds from the magnetic pyrochlore lattice family in which such quantum effects are expected is $MgTi_2O_4$ (d^1). Pure $MgTi_2O_4$ has been synthesized recently.[9] From the studies of the structural and transport properties of this compound it has been concluded that a metal-insulator type of phase transition takes place at about 260 K, which is accompanied by a structural transformation of a lattice from cubic to tetragonal.[9] The magnetic susceptibility decreases sharply below the phase transition temperature, which, together with the structural change, indicates the importance of the interaction between magnetic moments and the $MgTi_2O_4$ lattice. However, neither the magnetic ground state at low temperatures nor the origin of the phase transition has been determined up until now.

Many of the physical properties of spinel oxide $MgTi_2O_4$, including lattice dynamics, are unknown. Here we report the measurements of infrared and Raman spectra of $MgTi_2O_4$ in a wide temperature and frequency range, which are used to study the lattice dynamics in this compound. We have observed four Raman and two infrared active modes. The assignment of the observed modes is done using lattice dynamical calculations based on the shell model. The phase transition at about 250 K is manifested through an abrupt change of the reflectivity coefficient, by a plasma frequency decrease, as well as the appearance of new phonon modes.

II. EXPERIMENT

Powder samples of $MgTi_2O_4$ were prepared by a solid-state reaction of MgO, TiO_2, and Ti metal in an evacuated silica tube. Details on the preparation of the studied samples have been published elsewhere.[9]

Reflectivity spectra were measured from the powder pellets with a BOMEM DA-8 spectrometer. A DTGS pyroelectric detector was used to cover the frequency region from 80 to 600 cm^{-1}; a liquid-nitrogen cooled Hg-Cd-Te detector was used from 500 to 3000 cm^{-1}. Spectra were collected with 2 cm^{-1} resolution, with 1000 interferograms added for

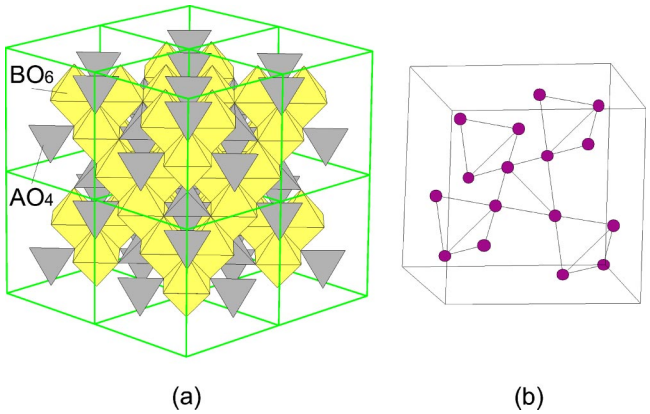

FIG. 1. (a) Schematic illustration of the AB_2O_4 spinel structure composed of AO_4 tetrahedra and BO_6 octahedra. (b) Three-dimensional network of corner-sharing tetrahedra formed by B cations (pyrochlore lattice).

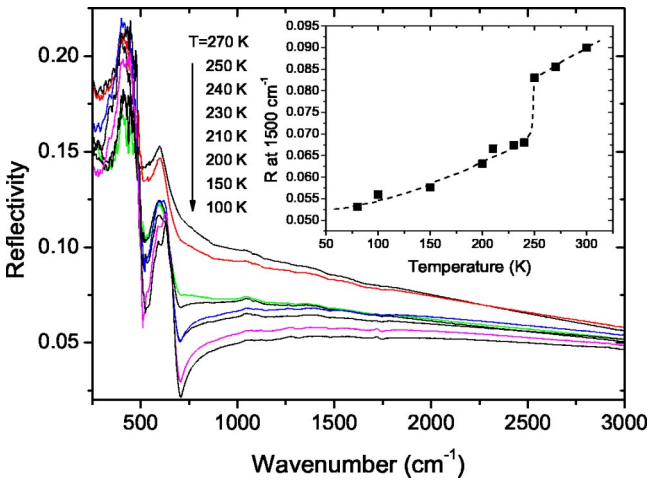

FIG. 2. Reflectivity spectra of the $MgTi_2O_4$ in the 250–3000 cm^{-1} spectral range at different temperatures. Inset: Reflectivity of $MgTi_2O_4$ at 1500 cm^{-1} as a function of temperature.

each spectrum. For low-temperature measurements a Janis STDA 100 cryostat was used.

The Raman spectra were measured using a micro-Raman system coupled to a DILOR triple spectrometer including a liquid-nitrogen cooled charge-coupled-device detector. The 514.5 nm line of an Ar-ion laser was used as excitation source. Low-temperature measurements were carried out in an Oxford continuous flow cryostat with window 0.5 mm thick. The laser beam was focused by a long working distance ($\sim$10 mm focal length) microscope objective (magnification 50×).

III. RESULTS AND ANALYSIS

The unit cell of $MgTi_2O_4$ consists of eight formula units, $Z=8$ (two formula units per primitive cell with 14 atoms in all). The Mg and Ti atoms occupy the tetrahedral ($8a$) and octahedral ($16d$) sites in the $Fd\bar{3}m(O_h^7)$ space group. The oxygen atoms are in ($32e$) site symmetry positions. The factor-group-analysis (FGA) yields

$$\begin{aligned}&(\mathrm{Mg})(T_d)\Gamma = F_{1u}+F_{2g},\\ &(\mathrm{Ti})(D_{3d})\Gamma = A_{2u}+E_u+2F_{1u}+F_{2u},\\ &(\mathrm{O})(C_{3v})\Gamma = A_{1g}+A_{2u}+E_g+E_u+F_{1g}+2F_{1u}+2F_{2g}\\ &\qquad +F_{2u}.\end{aligned}$$

Summarizing these representations and subtracting the acoustic (F_{1u}) and silent modes, we obtain the following irreducible representations of $MgTi_2O_4$ vibrational modes:

$$\Gamma^{opt.}_{MgTi_2O_4} = A_{1g}+E_g+3F_{2g}+4F_{1u}.$$

According to this analysis one can expect 5 Raman and 4 infrared active modes to be observed experimentally.

Figure 2 shows the reflectivity spectra of $MgTi_2O_4$ measured from powder samples at different temperatures in the spectral range from 250 to 3000 cm^{-1}. The common features of the reflectivity spectra, presented in Fig. 2, are two strong phonon bands peaked at about 420 and 600 cm^{-1}, and a free carrier (plasma) contribution. By lowering the temperature, the observed modes harden and, at the phase transition temperature, the reflectivity decreases abruptly (more than 10%) (see inset in Fig. 2). In addition, the strong phonon oscillators start to decompose into several modes at temperatures below 230 K. This is a consequence of the phase transition, represented by the change of the crystal structure and symmetry from cubic to tetragonal.[9] In order to extract the optical parameters of phonons and plasmons we applied a fitting procedure based on the double damping extended Drude model (DDD) for the dielectric function[10]:

$$\tilde{\epsilon}(\omega)=\epsilon_\infty\left[\prod_{j=1}^{n}\frac{\omega_{LO,j}^2-\omega^2-i\omega\gamma_{LO,j}}{\omega_{TO,j}^2-\omega^2-i\omega\gamma_{TO,j}}-\frac{\Omega_p^2-i(\gamma_p-\gamma_0)\omega}{\omega(\omega-i\gamma_0)}\right], \quad (1)$$

where $\omega_{TO(LO)_j}$ and $\gamma_{TO(LO)_j}$ are the TO (LO) mode frequency and linewidth of the jth oscillator, Ω_p is the plasma frequency, and γ_p is the linewidth of the plasma response at $\omega=\Omega_p$. The parameter γ_0 is the linewidth of the absorption centered at $\omega=0$. This model was commonly used for a wide group of oxide materials[10] including AB_2O_4 spinels also.[11] The best fit parameters are listed in Table I.

Figure 3 shows the reflectivity spectra, calculated using Eq. (1) with the parameters from Table I, compared to the experimental data in the 100–900 cm^{-1} spectral range at four different temperatures. Figure 4 shows the Raman spectra of $MgTi_2O_4$ at room temperature and 25 K.

The assignment of the observed modes is given with the help of lattice dynamical calculations (LDC) based on the shell model. We used here the lattice constant parameter value $a=8.507$ Å and internal oxygen parameter $u=0.2579$, which were obtained by calculating the minimum of the total energy of $MgTi_2O_4$ using density functional theory within the framework of the linearized augmented-plane-wave method.[12] Increasing u from its ideal value 0.25 moves the oxygen away from the nearest tetrahedral cation along [111] and equivalent directions, producing an expansion of the MgO_4 tetrahedra and contraction of the TiO_6 octahedra. The lattice dynamical calculations were performed using the GULP (general utility-lattice program) code.[13] In the shell model[14] used here, the lattice is considered as an assembly of polarizable ions, represented by massive point cores and massless shells, coupled by isotropic harmonic forces. The interacting potential includes contributions from Coulomb, polarization, and short-range interactions. The sum of the core and shell charges is equal to the formal charge of the ion in the lattice. The short-range potentials used for the shell-shell (oxygen-oxygen) and core-shell (metal-oxygen) interactions are of the Buckingham form:

$$V_{ij}=A_{ij}\exp(-r/\rho_{ij})-C_{ij}/r^6. \quad (2)$$

The Buckingham parameters were fitted using the experimental data including the lattice parameter, the static and high-frequency dielectric constants, the frequency of the A_{1g} Raman mode, and the TO frequencies of infrared optical phonons in $MgTi_2O_4$ crystal. The final values of our shell-model parameters are presented in Table II. The calculated and experimentally observed phonon frequencies of

TABLE I. Optical parameters (frequencies and linewidths in cm^{-1}) used to fit the reflectivity spectra of $MgTi_2O_4$.

	T (K)									
	300	270	250	240	230	210	200	150	100	80
ω_{TO_1}	406	434	421	462	455	461	443	452.5	454.6	466
ω_{LO_1}	480	491	474.4	497.4	493	497	496	496	496.5	492
ω_{TO_2}	578	582	611	604	614	622.5	623	631.5	640	649
ω_{LO_2}	604.4	666	637	643	654	661	661.5	669.5	665.4	674
ω_p	1153	992	984	920	891	798	758.5	667	653	392
ϵ_∞	1.21	1.21	1.68	1.69	1.69	1.98	2.07	2.14	2.31	2.31
γ_{TO_1}	123	141	109	118	103.5	101	108	97	101	80
γ_{LO_1}	158	91	127	86	76	67	65	52	41	63
γ_{TO_2}	121	143	90	100	98	101.4	92	92	90.5	82.5
γ_{LO_2}	201	212	97	112	87	76	61	50	40	58
γ_p	5505	5505	4522	4682	4482	3902	3523	3067	2202	2135
γ_0	1775	141	109	118	103.5	101	108	97	101	80

$MgTi_2O_4$ together with the mode assignment are summarized in Table III. As can be seen from Table III, the phonon frequencies obtained in our calculations are in rather well agreement with the experimentally observed.

IV. DISCUSSION

According to the FGA and the LDC we can expect 5 Raman and 4 infrared active modes to be observed in the experiment. In the case of the Raman spectra (Fig. 4), four modes at 335, 448, 493, and 628 cm^{-1} are observed, one less than theoretically predicted. The lowest energy Raman mode at 335 cm^{-1} originates mostly from Mg ion vibrations. All other Raman modes represent oxygen ion vibrations. The highest frequency mode of F_{2g} symmetry ($\omega_{calc.} = 644$ cm^{-1}, Table III) is probably of very low intensity. Because of that, and since the Raman scattering cross section in $MgTi_2O_4$ is very small, it was not possible to resolve it from the noise level. Besides Raman modes, a broad structure between 200 and 700 cm^{-1} is also present in Fig. 4. The intensity of this structure increases by lowering the temperature and shifts slightly to higher energy. The spin or polaronic excitations can produce such broad background structure, which is peaked at about 500 cm^{-1}. However, neither magnetic origin nor polaronic scattering scenario can be proved to be responsible for the appearance of this structure in the Raman spectra, due to lack of proper understanding of

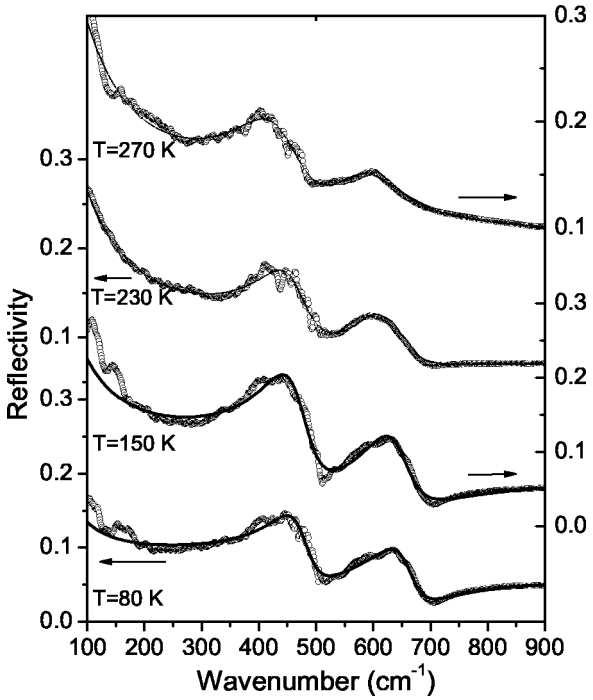

FIG. 3. Reflectivity spectra of $MgTi_2O_4$ sample in the 100–900 cm^{-1} spectral range at different temperatures. Experimental data are represented by circles; solid lines are calculated spectra using the DDD model, described in the text.

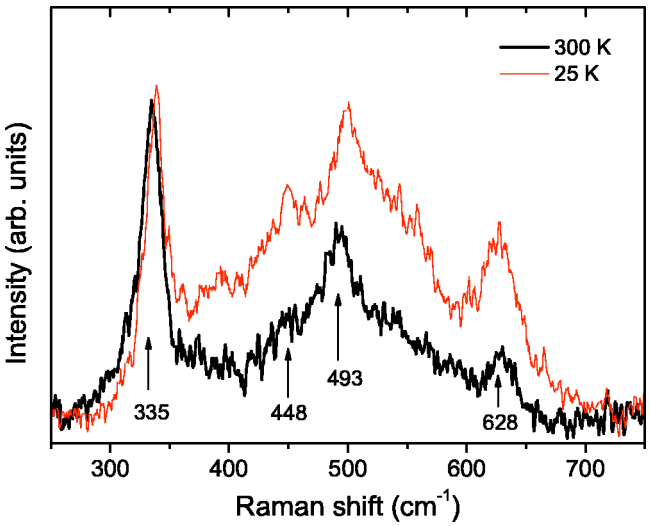

FIG. 4. Raman scattering spectra of a $MgTi_2O_4$ polycrystalline sample in the 250–750 cm^{-1} spectral range measured at 300 K (solid line) and 25 K (dotted line). The laser excitation wavelength was $\lambda_L = 514.5$ nm.

TABLE II. Model parameters for short-range interactions in $MgTi_2O_4$.

	A (eV)	ρ (Å)	C(eV Å^{-6})	$Y(\|e\|)$	k(eV Å^{-2})
Mg^{2+}	2911.1	0.2707	0.00	0.42	477.78
Ti^{3+}	1882.6	0.3097	0.00	1.23	58.71
O^{2-}	22764.3	0.1490	20.37	−2.48	41.75

the magnetic ground state and the carrier effective mass in this oxide.

Since the $MgTi_2O_4$ sample contains a slight amount (less than 5%) of (Mg,Ti) oxides[9] and due to the fact that the Raman scattering can be extremely sensitive to the presence of small amounts of insulating impurities in polycrystalline materials, we compared our spectra (Fig. 4) to the corresponding Raman spectra of MgO,[15,16] TiO_2,[17,18] and Ti_2O_3.[19] MgO crystallizes in the NaCl-type of crystal structure and the first-order Raman scattering is not allowed. However, when an impurity is introduced,[15] or if the particle size is small enough,[16] the selection rules are relaxed and observation of the first-order Raman spectra in MgO becomes possible. Ishikawa *et al.* revealed that two peaks at about 280 and 446 cm^{-1} appear in the Raman spectra of MgO microcrystals when the particle size is less than 100 nm. These modes are related to the peaks of the phonon density states in the MgO clusters. Raman spectra of $MgTi_2O_4$ (Fig. 4) do not present the 280 cm^{-1} mode. On the other hand, there is one weak mode at 448 cm^{-1}, which could be assigned as a MgO mode. However, since the particle size in $MgTi_2O_4$ is above 1 μm, we believe that the 448 cm^{-1} mode in Fig. 4 is an intrinsic $MgTi_2O_4$ mode.

For the synthesis of $MgTi_2O_4$ we used the rutile modification of TiO_2. This modification has the strongest Raman mode at about 612 cm^{-1} (A_{1g} symmetry mode), and the second in intensity mode at about 350 cm^{-1} (E_g).[17] We did not find these modes in Raman spectra in Fig. 4, and we did not observe the Raman modes of the anatase phase of TiO_2 at about 640 cm^{-1} (E_g) and 519 cm^{-1} (A_{1g}).[18] Finally, the strong Raman modes of Ti_2O_3 (Ref. 19) at 236, 279, and 350 cm^{-1} are also not detected in our spectra (see Fig. 4). Having all the above in mind, and since the frequencies of the Raman modes from Fig. 4 are very close to the frequencies of the corresponding modes of isostructural $LiTi_2O_4$,[20] we concluded that all Raman peaks assigned in Fig. 4 represent the lattice vibrational modes of pure $MgTi_2O_4$.

TABLE III. Observed and calculated phonon frequencies (in cm^{-1}) in $MgTi_2O_4$.

Symmetry	Activity	Calculated	Experiment
F_{1u}	Acoustic	0	-
F_{2u}	Silent	80	-
E_u	Silent	230	-
F_{1u}	Infrared	278	-
F_{1u}	Infrared	314	-
F_{2u}	Silent	319	-
F_{2g}	Raman	339	335
F_{1g}	Rotational	369	-
E_g	Raman	374	448
F_{1u}	Infrared	450	406
A_{2u}	Silent	470	
E_u	Silent	483	
F_{2g}	Raman	551	493
A_{2u}	Silent	611	
A_{1g}	Raman	628	628
F_{1u}	Infrared	635	578
F_{2g}	Raman	644	-

According to electrical resistivity measurements,[9] $MgTi_2O_4$ is probably a high electrical resistivity metal or semiconductor at room temperature. Below the phase transition temperature, it becomes an insulator. According to our infrared spectra, the plasma frequency shifts continuously to lower energy (Table I) by lowering the temperature between room and the phase transition $T_C = 250$ K. This indicates that $MgTi_2O_4$ may be a semiconductor at room temperature. The electronic structure calculation[12] indeed predicts the semiconducting high-temperature phase of $MgTi_2O_4$ with a gap value of about 2.8 eV. Consequently, this oxide undergoes a semiconductor-insulator transition at about 250 K. The same conclusion can be drawn from the temperature dependence of the electrical resistivity, which is given in Fig. 4 of Ref. 9. Below T_C, the plasma frequency and plasma dampings continue to decrease, in accordance with the electrical resistivity versus temperature dependence from Ref. 9.

Lattice dynamics calculations predict the frequencies of the 4 TO infrared active modes to be at about 278, 314, 450, and 635 cm^{-1}. Experimentally, we found only two oscillators at TO/LO frequencies 406/480 and 578/604 cm^{-1}. These oscillators represent oxygen ion vibrations. Two low-frequency infrared active modes (mostly Ti and Mg ion vibrations) were hardly observed in most spinels because of their low intensity. In our case, free carriers additionally screen these modes making them unobservable in our spectra.

The frequency versus temperature dependencies for optical parameters extracted from the fitting procedure (Table I, Fig. 3) are presented in Figs. 5(a)–5(f). As it can be seen from Figs. 5(a)–5(b) the $TO_{1(2)}/LO_{1(2)}$ mode frequencies of $MgTi_2O_4$ increase by lowering the temperature, with an abrupt change close to the phase transition. The phonon dampings, Figs. 5(d) and 5(e), decrease by lowering the temperature, indicating that the lattice instability is strongly reduced in the low-temperature phase. Moreover, the plasma frequency and damping show also nonmonotonic change close to the phase transition temperature, Figs. 5(c) and 5(f). The phonon and plasmon anomalies and the lattice instability coincide with the abrupt change of the electrical resistivity and magnetic phase transition temperature.[9] Figure 6 shows the normalized TO phonon dampings together with normalized magnetic susceptibility from Ref. 9. We found that TO_1 and TO_2 phonon broadenings map well the normalized magnetic susceptibility curve, indicating that the magnetic phase transition leaves a fingerprint in the lattice dynamics of $MgTi_2O_4$. As we mentioned above, the $MgTi_2O_4$ undergoes the phase transition from the metallic (semiconductor) to the

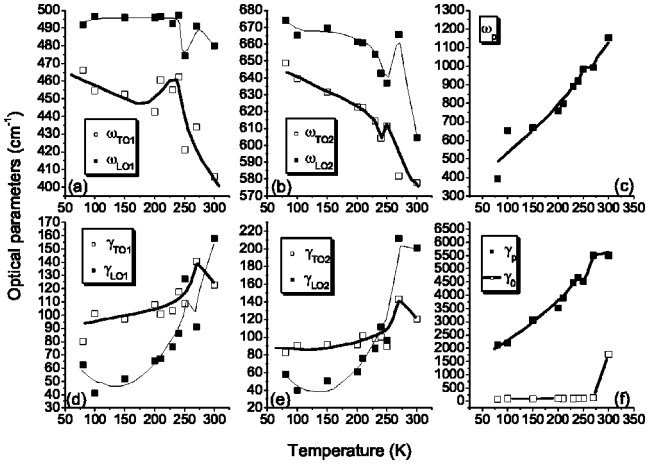

FIG. 5. Temperature dependence of phonon and plasmon parameters used in the fitting procedure of the reflectivity data. Lines are guide to the eyes.

insulator (*M-I*) state at about 250 K, which is the first observation of *M-I* transition without charge separation or charge order in the spinel compounds.[9] Usually, as in the case of manganites,[21] or pyroxenes,[22] if the orbital ordering or orbital dynamics is involved and/or responsible for the phase transition, then the changes of the magnetic and electric properties are accompanied with structural changes. The crystal structure of $MgTi_2O_4$ is built from TiO_6 octahedra, Fig. 1(a), which are mutually connected by common edges forming Ti-O chains. As we discussed in Ref. 22, the edge shared TiO_6 octahedra are predisposed to dimerization. We believe that some kind of orbital ordering/dimerization may also take place in the low-temperature phase of $MgTi_2O_4$.

The structural and symmetry changes in the low-temperature phase are also manifested by the appearance of new phonon modes, as illustrated in Fig. 7. The decomposition of the 600 cm^{-1} oscillator into several modes is clearly observed at temperatures lower than 210 K. Since the reflectivity measurements carried out on powder samples give good results for TO and LO mode frequencies in the case of

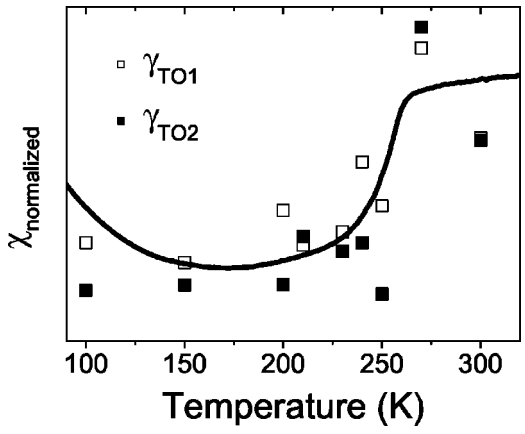

FIG. 6. Temperature dependence of the normalized damping of $TO_{1(2)}$ phonons together with the normalized magnetic susceptibility (solid line) of $MgTi_2O_4$, Ref. 9.

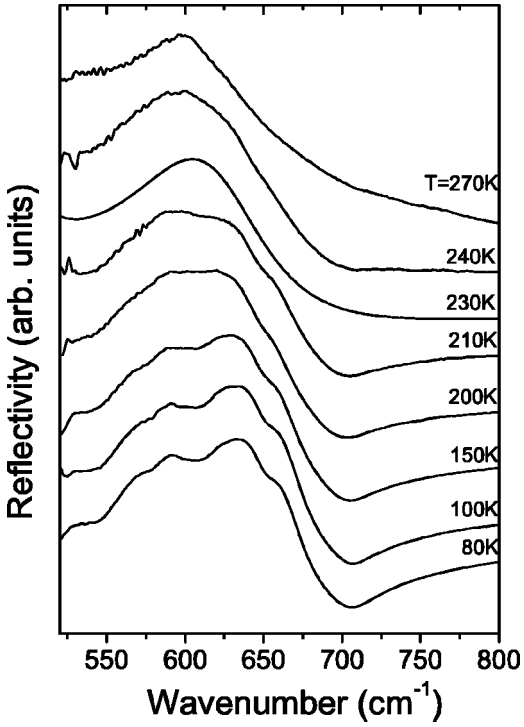

FIG. 7. Infrared reflectivity spectra of $MgTi_2O_4$ at different temperatures in the 500–800 cm^{-1} range.

isolated oscillators only, the fitting of the broad infrared band with many oscillators in the low-temperature phase does not have sense. Namely, two or more oscillators from different symmetries can appear as multipeak structure in the reflectivity spectra of powder samples.[23] Because of that, the assignment of the infrared-active modes in the low temperature phase of $MgTi_2O_4$ is practically impossible without crystal structure determination of this phase and polarized measurements on single crystals.

In conclusion, we have measured Raman scattering and reflectivity spectra of $MgTi_2O_4$ samples at different temperatures. We observed four (of five) Raman and two (of four) infrared active modes, predicted by factor-group analysis for cubic symmetry of $MgTi_2O_4$. In the Raman spectra the broad structure peaked at about 500 cm^{-1} increases its intensity by lowering the temperature. The assignment of the observed modes is done using lattice dynamical calculations based on the shell model. The phase transition at about 250 K is manifested through an abrupt change of the reflectivity coefficient as well as plasma frequency decrease and the appearance of new phonon modes. Analyzing the phonon frequency and damping versus temperature dependance we found that the magnetic phase transition leaves a fingerprint in the phonon dynamics of $MgTi_2O_4$.

ACKNOWLEDGMENTS

One of us (Z.V.P) thanks the Ministry for Education, Culture and Sport of Spain for financial support. This work was supported in part by the Serbian Ministry of Science and Technology under Project No. 1469.

[1] D.C. Johnston, H. Prakash, W.H. Zachariasen, and R. Viswanathan, Mater. Res. Bull. **8**, 777 (1973).
[2] S. Kondo, D.C. Johnston, C.A. Swenson, F. Borsa, A.V. Mahajan, L.L. Miller, T. Gu, A.I. Goldman, M.B. Maple, D.A. Gajewski, E.J. Freeman, N.R. Dilley, R.P. Dickey, J. Merrin, K. Kojima, G.M. Luke, Y.J. Uemura, O. Chmaissem, and J.D. Jorgensen, Phys. Rev. Lett. **78**, 3729 (1997).
[3] N. Fujiwara, H. Yasuoka, and Y. Ueda, Phys. Rev. B **57**, 3539 (1998).
[4] C. Urano, M. Nohara, S. Kondo, F. Sakai, H. Takagi, T. Shiraki, and T. Okubo, Phys. Rev. Lett. **85**, 1052 (2000).
[5] K. Matsuno, T. Katsufuji, S. Mori, Y. Moritomo, A. Machida, E. Nishibori, M. Takata, M. Sakata, N. Yamamoto, and H. Takagi, J. Phys. Soc. Jpn. **70**, 1456 (2001).
[6] B. Canals and C. Lacroix, Phys. Rev. Lett. **80**, 2933 (1998).
[7] Y. Yamashita and K. Ueda, Phys. Rev. Lett. **85**, 4960 (2000).
[8] O. Tchernyshyov, R. Moessner, and S.L. Sondhi, Phys. Rev. Lett. **88**, 67203 (2002).
[9] M. Isobe and Y. Ueda, J. Phys. Soc. Jpn. **71**, 1848 (2002).
[10] F. Gervais, Mater. Sci. Eng., R. **39**, 29 (2002).
[11] P. Thibaudeau and F. Gervais, J. Phys.: Condens. Matter **14**, 3543 (2002).
[12] D. Olguin *et al.* (unpublished).
[13] J.D. Gale, J. Chem. Soc., Faraday Trans. **93**, 69 (1992).
[14] B.G. Dick and A.W. Overhauser, Phys. Rev. **112**, 90 (1958).
[15] S. Guha, Phys. Rev. B **21**, 5808 (1980).
[16] K. Ishikawa, N. Fujima, and H. Komura, J. Appl. Phys. **57**, 973 (1985).
[17] P. Merle, J. Pascual, J. Camassel, and H. Mathieu, Phys. Rev. B **4**, 1617 (1980).
[18] M. Mikami, S. Nakamura, O. Kitao, and H. Arakawa, Phys. Rev. B **66**, 155213 (2002).
[19] S.H. Shin, R.L. Aggarwal, B. Lax, and J.M. Honig, Phys. Rev. B **9**, 583 (1974).
[20] W.N. Liu, W. Hayes, M. Kurmoo, M. Dalton, and C. Chen, Physica C **235-240**, 1203 (1994).
[21] J. van den Brink, G. Khaliullin, and D. Khomskii, cond-mat/0206053 (unpublished).
[22] M.J. Konstantinović, J. van den Brink, Z.V. Popović, M. Isobe, and Y. Ueda, cond-mat/0210191 (unpublished).
[23] Z.V. Popović, M.J. Konstantinović, R. Gajić, V.N. Popov, M. Isobe, Y. Ueda, and V.V. Moshchalkov, Phys. Rev. B **65**, 184303 (2002).